Title
PHOTOMESON PRODUCTION FROM HYDROGEN AND DEUTERIUM

Permalink
https://escholarship.org/uc/item/4mw043hr

Authors
Kenney, Robert W.
Khapp, Edward A.
Perez-Mendez, Victor
et al.

Publication Date
1960-11-28

UCRL 9491

UNIVERSITY OF CALIFORNIA

Ernest O. Lawrence Radiation Laboratory

BERKELEY, CALIFORNIA

for publication in Physical Review

UCRL-9491
Limited distribution

UNIVERSITY OF CALIFORNIA
Lawrence Radiation Laboratory
Berkeley, California

Contract No. W-7405-eng-48

PHOTOMESON PRODUCTION FROM HYDROGEN AND DEUTERIUM

Robert W. Kenney, Edward A. Knapp, Victor Perez-Mendez,
and Walton A. Perkins

November 28, 1960

PHOTOMESON PRODUCTION FROM HYDROGEN AND DEUTERIUM

Robert W. Kenney, Edward A. Knapp, Victor Perez-Mendez,
and Walton A. Perkins

Lawrence Radiation Laboratory
University of California
Berkeley, California

November 28, 1960

ABSTRACT

The relative yields of positive pions produced from hydrogen and deuterium by the 340-Mev bremsstrahlung beam of the Berkeley synchrotron have been measured in the laboratory system at angles of 20, 40, and 60 deg, and at pion energies ranging from 45 to 145 Mev. The ratio of the relative yields of pions from deuterium and hydrogen was roughly constant as a function of angle, but decreased monotonically with pion energy from a value of 0.90 ± 0.05 at 45 Mev to a value of 0.55 ± 0.07 at 145 Mev.

Comparison with the phenomenological theory of Chew and Lewis indicates a gradual change from nucleon spin flip near threshold to no-spin-flip transitions above 140 Mev. Comparison with Uretsky's calculation involving final states shows fair agreement with plane-wave and shape-independent approximations. Poor agreement with the zero-range approximation shows that final-state interactions are important in the theory of deuteron photopion production.

PHOTOMESON PRODUCTION FROM HYDROGEN AND DEUTERIUM[*]

Robert W. Kenney, Edward A. Knapp,[†] Victor Perez-Mendez,[§]
and Walton A. Perkins[**]

Lawrence Radiation Laboratory
University of California
Berkeley, California

November 28, 1960

I. INTRODUCTION

The basic reactions $\gamma + p \rightarrow \pi^+ + n$ and $\gamma + n \rightarrow \pi^- + p$ have been studied by many theoretical and experimental workers.[1] The first reaction is directly accessible to experiment and has been more extensively investigated than the second reaction which is most simply observed in data from $\gamma + d \rightarrow \pi^- + 2p$. This interpretation of deuterium-target data requires knowledge of nucleon initial and final states, the latter being the less well known. For threshold production, coulomb corrections become important and are difficult to handle. Accordingly, many workers have studied the reactions $\gamma + p \rightarrow \pi^+ + n$ and $\gamma + d \rightarrow \pi^+ + 2n$.[1] One motivation for this study is to understand more fully the pion photoproduction on a bound proton. In principle, if one knows the matrix elements for positive photopion production on protons, the deuterium positive photopion production can also be calculated. Taking this approach,

---

[*] This work was done under the auspices of the U. S. Atomic Energy Commission.

[†] Present address: Los Alamos Scientific Laboratory, Los Alamos, New Mexico.

[§] Present address: The Hebrew University, Jerusalem, Israel.

[**] Present address: Lawrence Radiation Laboratory, University of California, Livermore, California.

Uretsky has utilized the dispersion theory of Chew et al.[3] for the $\gamma + p \rightarrow \pi^+ + n$ reaction. He has taken this theory with various assumed final-state interactions of the two neutrons in the deuterium reaction and has calculated the expected ratio

$$\left(\frac{d\sigma}{d\Omega}\right)_D \Big/ \left(\frac{d\sigma}{d\Omega}\right)_H$$

for π^+ photoproduction from deuterium and hydrogen, where $(d\sigma/d\Omega)_D$ and $(d\sigma/d\Omega)_H$ are the differential cross sections for deuterium and hydrogen, respectively. It is clear that the final-state nucleon interaction is important. Our data are compared to Uretsky's results.

When the production of deuterium positive photopions is understood satisfactorily, the reaction $\gamma + d \rightarrow \pi^- + 2p$ can be more easily interpreted to give information on the basic reaction, $\gamma + n \rightarrow \pi^- + p$. In the threshold region, satisfactory handling of the coulomb corrections is also required. Baldin has treated the coulomb corrections with some measure of success.[4] However, we restrict our attention in this work to the π^+ production from hydrogen and deuterium. Some insight into the nucleon spin-flip probability in π^+ photoproduction in deuterium is obtained from the early calculations of Chew and Lewis[5] and Lax and Feshbach.[6] They use the impulse approximation and assume that the interaction can be written $H = L + \vec{\sigma} \cdot \vec{K}$, where $\vec{K}$ and L are the spin-flip and no-spin-flip amplitudes, respectively. White et al. have evaluated the Chew-Lewis calculations for the ratio

$$\left(\frac{d\sigma}{d\Omega}\right)_D \Big/ \left(\frac{d\sigma}{d\Omega}\right)_H$$

as a function of pion laboratory energy.[7] Our data are compared to their result.

II. METHOD AND EXPERIMENTAL APPARATUS

Basic information on photopion production includes the incident photon energy, k. Using the two-body final state in the reaction $\gamma + p \rightarrow \pi^+ + n$, we can determine k if two final-state kinematic parameters are known, e.g. θ_π and T_π. The three-body final state in the reaction $\gamma + d \rightarrow \pi^+ + 2n$ allows no such simple analysis. Simplicity requires that we observe only the laboratory parameters θ_π and T_π for both reactions, and in comparing results with theory, that suitable averages over the photon energy spectrum be taken in the theory for the deuterium production. The function of interest in this work is the ratio of π^+ yields from deuterium and hydrogen versus pion energy at a given angle.

The 340-Mev bremsstrahlung beam of the Berkeley synchrotron traversed a vacuum-insulated target consisting of liquid hydrogen contained in a thin-walled Mylar vessel as shown in Fig. 1. Details of this target structure are given elsewhere.[8] Without disturbing the geometry, liquid hydrogen could be introduced directly into the target, or deuterium gas could be liquified in a condenser integral with the target apparatus and introduced interchangeably with hydrogen. The photon flux was monitored by a thick-walled copper ionization chamber (Cornell chamber).[9]

The pions produced in the target were detected at laboratory angles of 20, 40, and 60 deg by a pion telescope as shown in Fig. 1. The pions were identified by their π-μ decay signature after traversing scintillators 1, 2, and 3 and the copper absorber and stopping in scintillator 4. A μ decay pulse in scintillator 4, observed in delayed coincidence with the pion-arrival pulses from the preceeding scintillators, was the criterion for positive-pion identification. Its energy was calculated from the copper-absorber thickness, and electronic cancellation of unwanted high-energy traversals is effected when long-range particles pass through the antiscintillator (No. 5). The scintillators were approximately 3 by 3 by 1/4-in. -thick, the stopping scintillator (No. 4) was 1-in. -thick, and the antiscintillator (No. 5) geometry was adequate to detect all particles transmitted by the entire telescope, even though they scattered through 90 deg in scintillator No. 5. The electronics, shown in Fig. 2, have been described in detail elsewhere.[10]

III. RESULTS AND DISCUSSION

The ratio of positive-pion yields at a given angle and pion energy can be calculated nearly free from systematic errors because it is only the ratio and not the absolute yields which is of interest. Counter-telescope efficiency and solid angle remain fixed, as does the target geometry, for both hydrogen and deuterium runs.

The ratio

$$\left(\frac{d\sigma}{d\Omega}\right)_D \Big/ \left(\frac{d\sigma}{d\Omega}\right)_H = \frac{Y_D}{Y_H} \quad \frac{\rho_H}{\rho_D} \quad \frac{M_D}{M_H}$$

is therefore calculated completely independently of all geometrical factors. Results are listed in Table I. Here Y_D and Y_H are measured net counting rates, ρ_D and ρ_H are the tabulated densities, and M_D and M_H the atomic weights of deuterium and hydrogen, respectively. In finding the net counting rates Y_D and Y_H, a measured "target-empty" background was subtracted. The residual gas present in the target was accounted for. Small uncertainties exist due to errors in measured densities of liquid hydrogen and deuterium, and to small concentrations of helium and hydrogen impurities in the deuterium. These small errors were ignored in comparison with the counting errors (standard deviations) which are listed in Table I.

The results are plotted in Fig. 3 along with the three theoretical curves calculated by Dr. J. Uretsky[2] of this laboratory. The dispersion

Table I. Ratios of positive-pion yields at $\theta_L = 20$, 40, and 60 deg. for various pion energies

T_π	$\left(\frac{d\sigma}{d\Omega}\right)_D \Big/ \left(\frac{d\sigma}{d\Omega}\right)_H$		
(Mev)	θ_L = 20 deg	θ_L = 40 deg	θ_L = 60 deg
45		0.89 ± 0.05	0.90 ± 0.05
65	0.87 ± 0.07	0.78 ± 0.05	0.89 ± 0.05
85	0.79 ± 0.07	0.71 ± 0.04	0.77 ± 0.04
105	0.86 ± 0.08	0.75 ± 0.05	0.69 ± 0.04
125	0.67 ± 0.06	0.70 ± 0.06	0.57 ± 0.04
145	0.54 ± 0.06	0.54 ± 0.08	

relation theory of Chew et al.[3] was used along with the Hulthen wave function for the deuteron. Three different assumptions were made for the final-state two-neutron interaction. A plane-wave approximation was first made in which no interaction exists. The result is shown as the full curves in Fig. 3. Then ^1S scattering in the final state was considered under two assumptions. The di-neutron wave function was assumed to have its asymptotic form everywhere (zero-range approximation); the result is shown in Fig. 3. Finally, a more realistic "shape-independent" di-neutron wave function was chosen. It was similar to the zero-range approximation, but was required to remain finite for vanishing separation of the two neutrons. This result is also shown in Fig. 3. The S-state neutron scattering parameters which gave the best fit are $a_S = 17.10^{-13}$ cm and $r_{0_S} = 2.6.\ 10^{-13}$ cm. It was found that for small pion energies and small angles, the S interaction contributes as much as 15% to the deuteron cross section in addition to the basic plane-wave approximation.

A χ^2 analysis of the data and the three curves was made to determine the best fit in a quantitative manner. Table II gives values of χ^2 divided by the number of degrees of freedom for all cases.

Table II. χ^2 divided by degrees of freedom for data of Fig. 3

θ_L (deg)	Plane wave	Shape indep.	Zero range
20	2.3	2.08	7.07
40	2.3	2.7	14.9
60	3.3	5.7	14.2

The plane-wave and shape-independent approximations give nearly the same results, and there is no clear choice between them. At $\theta_L = 60$ deg, the plane-wave approximation is better, but neither approximation is a particularly good fit based upon the usual χ^2 test criteria. The fits at

20 and 40 deg are marginal also. We conclude that the zero-range approximation is significantly poorer than either the plane-wave or shape-independent approximations.

The data at θ_L = 20 deg are compared with the somewhat older impulse-approximation calculations of Chew and Lewis[5] in order to discuss the proton spin flip probability in the deuterium production. It is clear that at the positive photopion threshold for deuterium, the nucleon (proton) must flip its spin in order to enter a ^1S final state with the neutron. At somewhat higher energy, the nucleon(proton) may retain its spin direction and enter a ^3P final state with the neutron. This behavior is seen to occur in Fig. 4 by comparing the observed ratio with the curves $\gamma^2 = 0$ (spin flip) and $\gamma^2 = 1$ (no spin flip). At 140 Mev, the data are consistent with a high probability of no nucleon spin flip, and the data at energies below 100 Mev show that the spin-flip probability is approximately unity.

ACKNOWLEDGMENTS

The collaboration and encouragement of Professor A. Carl Helmholz throughout the course of this work is gratefully acknowledged. Our thanks are due Dr. J. Uretsky for many fruitful discussions on some theoretical aspects of the problem. Our appreciation is extended to Mr. R. Johnson and the synchrotron crew for their cooperation during the runs. The help of Mr. R. Kurz in the final phases of the experiment is acknowledged with thanks.

References

1. H. A. Bethe and F. de Hoffman, Mesons and Fields, Vol. II, (Row-Peterson and Co., Evanston, Illinois) 1955.
2. J. Uretsky, Bull. Am. Phys. Soc. II, 3, 12 (1958).
3. G. F. Chew, M. L. Goldberger, F. E. Low, and Y. Nambu, Phys. Rev. 106, 1345 (1957).
4. A. M. Baldin, Nuovo cimento 8, 569 (1958).
5. G. F. Chew and H. W. Lewis, Phys. Rev. 84, 779 (1951).
6. M. Lax and H. Feshbach, Phys. Rev. 88, 509 (1952).
7. R. S. White, M. J. Jakobson, and A. G. Schulz, Phys. Rev. 88, 836 (1952).
8. R. S. Hickman, R. W. Kenney, R. C. Mathewson, and R. A. Perkins, Rev. Sci. Instr. 30, 983 (1959).
9. F. L. Loeffler, T. R. Palfrey, G. W. Tautfest, Nucl. Instr. and Methods 5, 50 (1959).
10. E. A. Knapp, R. W. Kenney, and V. Perez-Mendez, Phys. Rev. 114, 605 (1959).

Figure Legends

Fig. 1. Counter telescope.

Fig. 2. Block diagram of the electronics.

Fig. 3. Positive-pion yield at θ_L = 20, 40, and 60 deg vs pion energy.

Fig. 4. Positive-pion yield at θ_L = 20 deg vs pion energy. The curves are from White et al. for θ_L = 25 deg. For spin flip, $\gamma^2 = 0$; for no spin flip, $\gamma^2 = 1$.

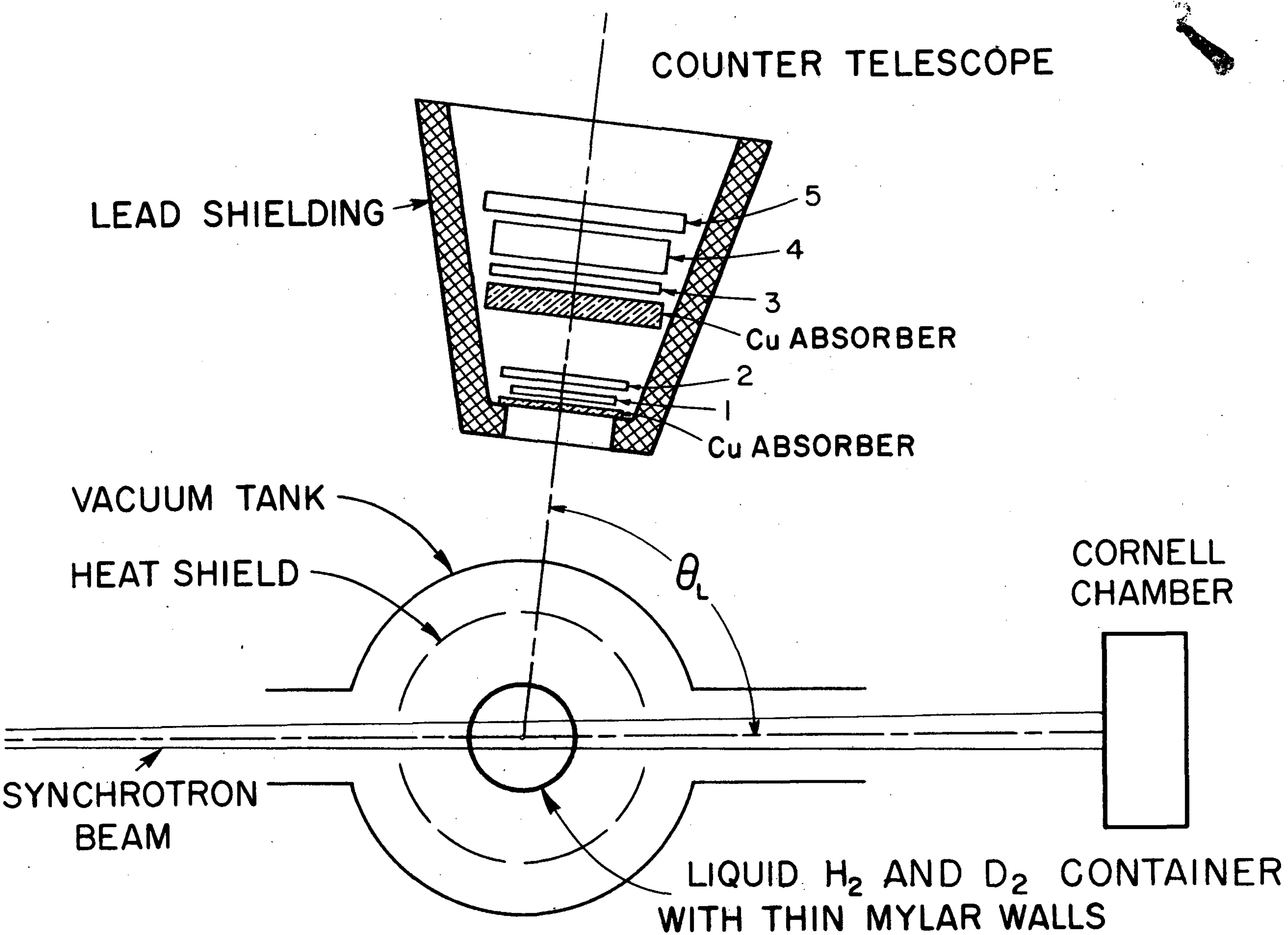
COUNTER TELESCOPE
LEAD SHIELDING
5
4
3
Cu ABSORBER
2
1
Cu ABSORBER
VACUUM TANK
HEAT SHIELD
θ_L
CORNELL
CHAMBER
SYNCHROTRON
BEAM
LIQUID H_2 AND D_2 CONTAINER
WITH THIN MYLAR WALLS

Fig. 1

50,674-1

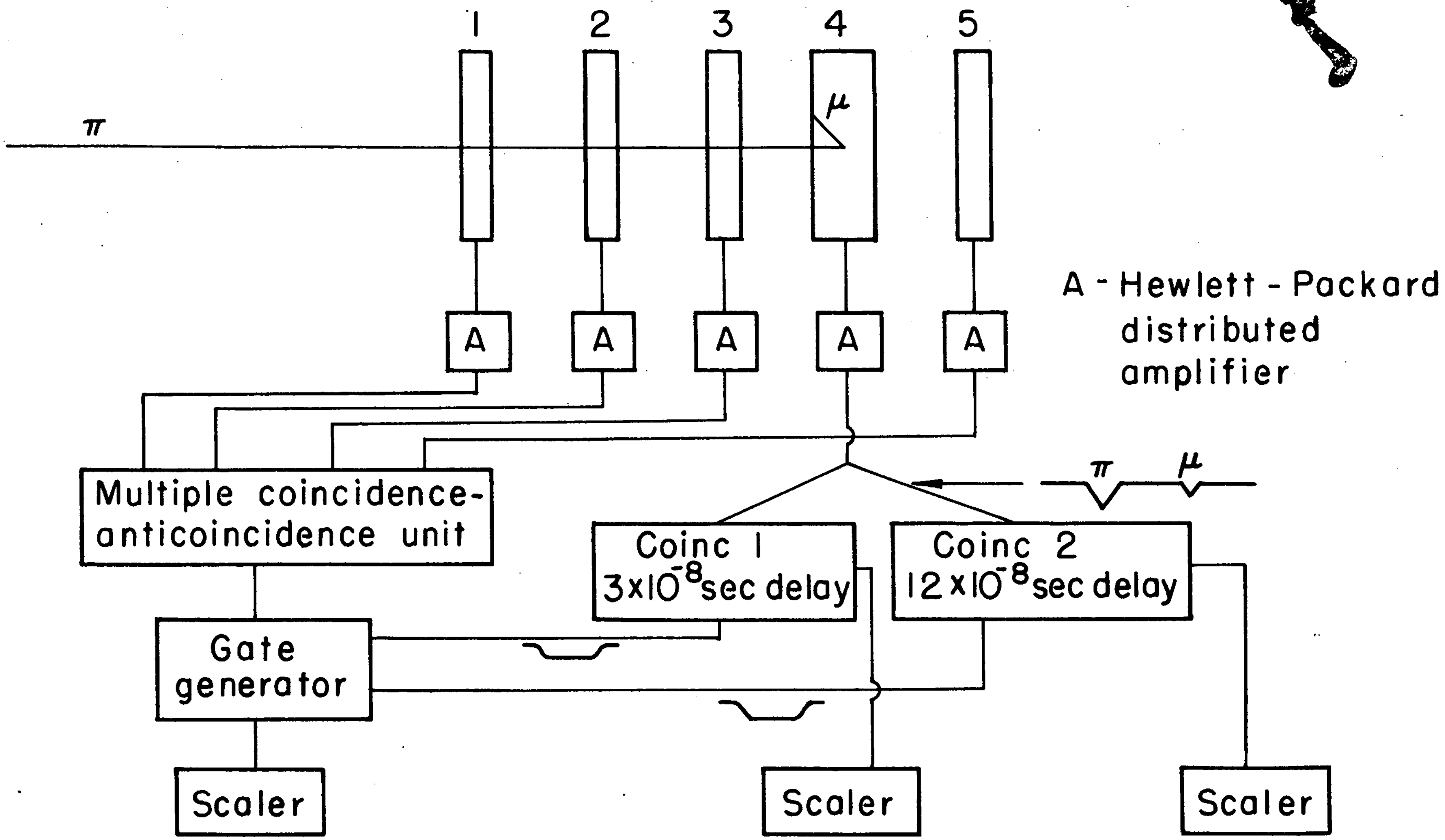
1
2
3
4
5
π
μ
A
A
A
A
A
A - Hewlett - Packard distributed amplifier
π
μ
Multiple coincidence-anticoincidence unit
Coinc 1 3x10⁻⁸ sec delay
Coinc 2 12x10⁻⁸ sec delay
Gate generator
Scaler
Scaler
Scaler

Fig. 2

58683-1

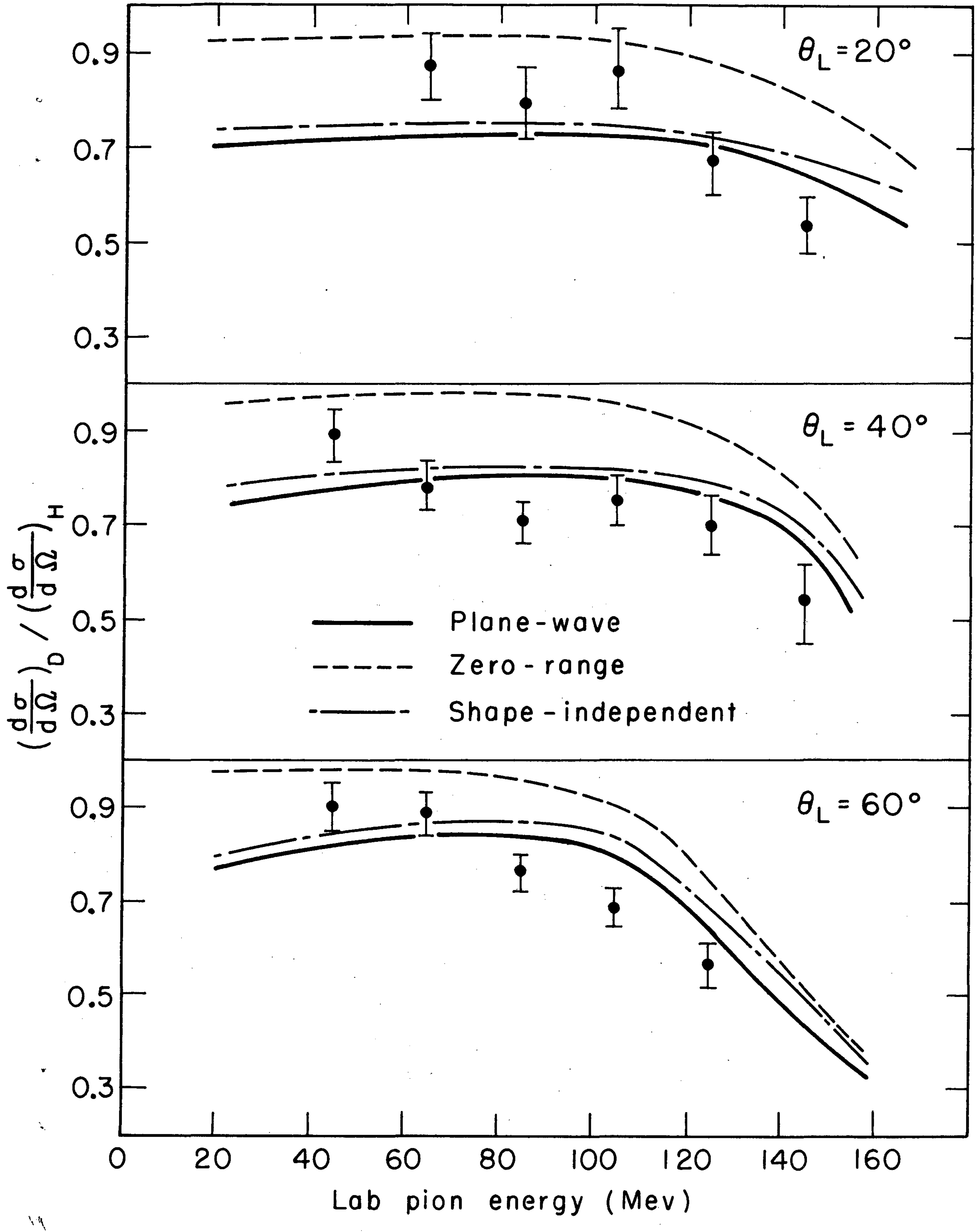

0.9
0.7
0.5
0.3
$\theta_L = 20°$
$\theta_L = 40°$
$\theta_L = 60°$
$\left(\frac{d\sigma}{d\Omega}\right)_D / \left(\frac{d\sigma}{d\Omega}\right)_H$
Plane-wave
Zero-range
Shape-independent
0
20
40
60
80
100
120
140
160
Lab pion energy (Mev)

Fig 3

58682-1

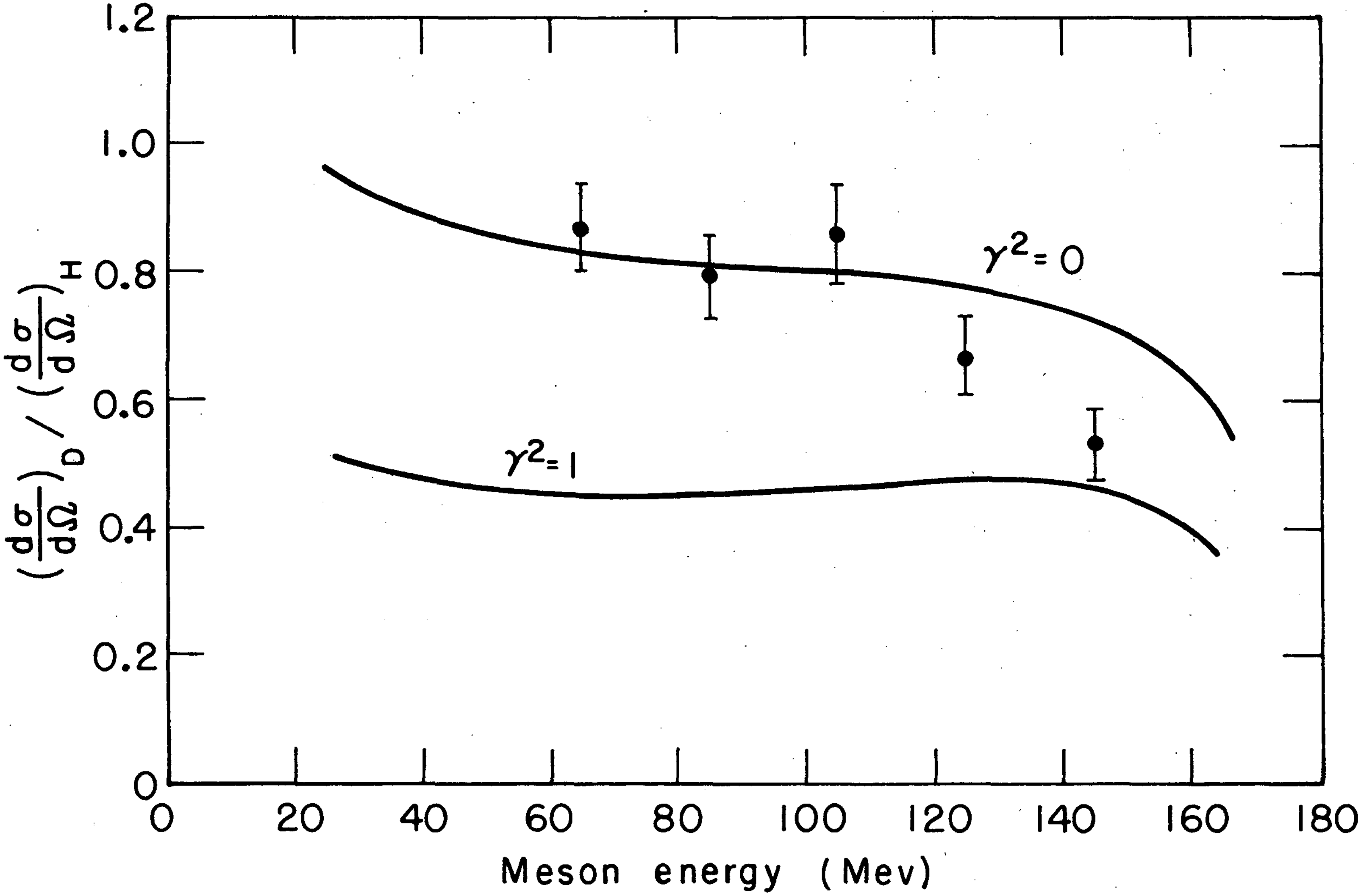
1.2
1.0
0.8
0.6
0.4
0.2
0
$\left(\frac{d\sigma}{d\Omega}\right)_D / \left(\frac{d\sigma}{d\Omega}\right)_H$
$\gamma^2 = 0$
$\gamma^2 = 1$
0
20
40
60
80
100
120
140
160
180
Meson energy (Mev)

Fig. 4

58681-1